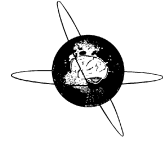




Contents lists available at ScienceDirect

Clinical Neurophysiology

journal homepage: www.elsevier.com/locate/clinph

Whole-body fasciculation detection in amyotrophic lateral sclerosis using motor unit MRI (MUMRI)

Linda Heskamp^{a,*}, Matthew G. Birkbeck^{a,b,c}, Julie Hall^{a,d}, Ian.S. Schofield^a, James Bashford^e, Timothy L. Williams^f, Hugo M. De Oliveira^{a,f}, Roger G. Whittaker^{a,f,1,*}, Andrew M. Blamire^{a,1}

^aNewcastle University Translational and Clinical Research Institute (NUTCRI), Newcastle University, Newcastle Upon Tyne, United Kingdom

^bNewcastle Biomedical Research Centre (BRC), Newcastle University, Newcastle Upon Tyne, United Kingdom

^cNorthern Medical Physics and Clinical Engineering, Freeman Hospital, Newcastle Upon Tyne NHS Foundation Trust, Newcastle Upon Tyne, United Kingdom

^dDepartment of Neuroradiology, Royal Victoria Infirmary, Newcastle Upon Tyne, United Kingdom

^eMaurice Wohl Clinical Neuroscience Institute, Institute of Psychiatry, Psychology and Neuroscience, King's College London, United Kingdom

^fDirectorate of Clinical Neurosciences, Royal Victoria Infirmary, Newcastle Upon Tyne, United Kingdom

HIGHLIGHTS

- Whole body motor unit MRI (MUMRI) offers a sensitive and non-invasive method to image fasciculation in multiple body regions.
- Whole body MUMRI fasciculation rates correlated with single channel surface EMG fasciculation rates.
- MUMRI discriminated well between ALS patients and healthy people for proximal limb and paraspinal muscles, but not the tongue.

ARTICLE INFO

Article history:

Accepted 7 February 2024

Available online

Keywords:

Amyotrophic lateral sclerosis

Fasciculation

Motor unit MRI

Skeletal muscle

Diffusion weighted MRI

ABSTRACT

Objective: Compare fasciculation rates between amyotrophic lateral sclerosis (ALS) patients and healthy controls in body regions relevant for diagnosing ALS using motor unit MRI (MUMRI) at baseline and 6 months follow-up, and relate this to single-channel surface EMG (SEMG).

Methods: Tongue, biceps brachii, paraspinals and lower legs were assessed with MUMRI and biceps brachii and soleus with SEMG in 10 healthy controls and 10 patients (9 typical ALS, 1 primary lateral sclerosis [PLS]).

Results: MUMRI-detected fasciculation rates in typical ALS patients were higher compared to healthy controls for biceps brachii ($2.40 \pm 1.90 \text{ cm}^{-3}\text{min}^{-1}$ vs. $0.04 \pm 0.10 \text{ cm}^{-3}\text{min}^{-1}$, $p = 0.004$), paraspinals ($1.14 \pm 1.61 \text{ cm}^{-3}\text{min}^{-1}$ vs. $0.02 \pm 0.02 \text{ cm}^{-3}\text{min}^{-1}$, $p = 0.016$) and lower legs ($1.42 \pm 1.27 \text{ cm}^{-3}\text{min}^{-1}$ vs. $0.13 \pm 0.10 \text{ cm}^{-3}\text{min}^{-1}$, $p = 0.004$), but not tongue ($1.41 \pm 1.94 \text{ cm}^{-3}\text{min}^{-1}$ vs. $0.18 \pm 0.18 \text{ cm}^{-3}\text{min}^{-1}$, $p = 0.556$). The PLS patient showed no fasciculation. At baseline, 6/9 ALS patients had increased fasciculation rates compared to healthy controls in at least 2 body regions. At follow-up every patient had increased fasciculation rates in at least 2 body regions. The MUMRI-detected fasciculation rate correlated with SEMG-detected fasciculation rates ($\tau = 0.475$, $p = 0.006$).

Conclusion: MUMRI can non-invasively image fasciculation in multiple body regions and appears sensitive to disease progression in individual patients.

Significance: MUMRI has potential as diagnostic tool for ALS.

© 2024 International Federation of Clinical Neurophysiology. Published by Elsevier B.V. This is an open access article under the CC BY license (<http://creativecommons.org/licenses/by/4.0/>).

Abbreviations: ALS, Amyotrophic lateral sclerosis; ALS-FRS, ALS Functional Rating Scale; DW, Diffusion weighted; FVC, Forced Vital Capacity; GL, Gastrocnemius lateralis; GM, Gastrocnemius medialis; MRI, Magnetic resonance imaging; MUMRI, Motor unit MRI; PER, Peroneus longus; PGSE, Pulsed gradient spin-echo; PLS, Primary lateral sclerosis; SD, Standard deviation; SEMG, Surface EMG; SOL, Soleus; SPiQE, Surface Potential Quantification Engine; TA, Tibialis anterior; TP, Tibialis posterior.

* Corresponding authors at: Newcastle University Translational and Clinical Research Institute (NUTCRI), Newcastle University, Newcastle Upon Tyne, United Kingdom.

E-mail addresses: linda.heskamp@newcastle.ac.uk (L. Heskamp), Matt.Birkbeck@newcastle.ac.uk (M.G. Birkbeck), julie.hall@nhs.net (J. Hall), ian.schofield@newcastle.ac.uk (I.S. Schofield), james.bashford@kcl.ac.uk (J. Bashford), tim.williams8@nhs.net (T.L. Williams), hugo.oliveira@newcastle.ac.uk (H.M. De Oliveira), roger.whittaker@newcastle.ac.uk (R.G. Whittaker), andrew.blamire@newcastle.ac.uk (A.M. Blamire).

¹ Joint senior author.

<https://doi.org/10.1016/j.clinph.2024.02.016>

1388-2457/© 2024 International Federation of Clinical Neurophysiology. Published by Elsevier B.V.

This is an open access article under the CC BY license (<http://creativecommons.org/licenses/by/4.0/>).

Please cite this article as: L. Heskamp, M.G. Birkbeck, J. Hall et al., Whole-body fasciculation detection in amyotrophic lateral sclerosis using motor unit MRI (MUMRI), *Clinical Neurophysiology*, <https://doi.org/10.1016/j.clinph.2024.02.016>

1. Introduction

In patients with amyotrophic lateral sclerosis (ALS) the typical interval from symptom onset to diagnosis is 12 months (Househam and Swash, 2000; Paganoni et al., 2014; Palese et al., 2019; Sennfalt et al., 2022), a time frame that has not changed despite increased awareness, improvements in healthcare access and decades of research. This delays access to multi-disciplinary care and clinical trials for a patient group with a median survival of only 30 months from disease onset (Feldman et al., 2022; Hardiman et al., 2011; Kiernan et al., 2011; Westeneng et al., 2018).

The most recent diagnostic guidelines (Gold Coast criteria) require the presence of upper and lower motor neuron dysfunction in at least one body region, or lower motor neuron dysfunction in at least two body regions (Shefner et al., 2020). Body regions are defined based on their innervation level, *i.e.* bulbar, cervical, thoracic and lumbosacral. The Gold Coast criteria emphasise the importance of fasciculation as an early hallmark of lower motor neuron dysfunction (de Carvalho and Swash, 2013), with fasciculation now accepted to be equivalent to fibrillation potentials and positive sharp waves in muscles with chronic neurogenic signs.

Fasciculation is defined as the pathological spontaneous contraction of motor units caused by instability of reinnervating motor units or supraspinal hyperexcitability (de Carvalho et al., 2017). In routine care, fasciculation is detected by clinical examination and needle EMG; however this technique is invasive and has limited coverage (de Carvalho et al., 2017; Paganoni et al., 2014). Increasingly, ultrasound is entering clinical practice as it offers a simple, easy and accessible way to assess fasciculation in a subset of muscles (Hobson-Webb and Simmons, 2019; Misawa et al., 2011). Ultrasound is currently the most sensitive technique for ALS diagnosis based on fasciculation; if fasciculation is detected in 3 or more muscles of the predefined subset, ALS can be diagnosed with a sensitivity of 86% and specificity of 96% (Fukushima et al., 2022). Single channel surface EMG has been used extensively to study the pathophysiology of fasciculation and is available in every neurophysiology clinic (de Carvalho et al., 2015; de Carvalho and Swash, 2016; Mateen et al., 2008). More recently, high-density surface EMG (SEMG) has been proposed (Tamborska et al., 2020). However, both ultrasound and SEMG are largely limited to superficial muscles and high density SEMG is not yet widely available.

Recently, we developed motor unit magnetic resonance imaging (MUMRI) as a non-invasive technique to detect fasciculation (Steidle and Schick, 2015; Whittaker et al., 2019). MUMRI uses a pulsed gradient spin-echo (PGSE) diffusion weighted (DW) sequence available on any modern magnetic resonance imaging (MRI) scanner in which motor unit contractions manifest as transient signal voids within skeletal muscles. A preliminary study in four ALS patients showed that MUMRI could non-invasively detect significantly increased fasciculation rates compared to healthy controls, but this study was limited to the lower leg on one side only (Whittaker et al., 2019). The aim of the present study was to compare fasciculation rates between ALS patients and healthy controls in all four body regions relevant to the diagnosis of ALS using MUMRI at baseline and after 6 months and relate this to single-channel SEMG measurements.

2. Material and methods

2.1. Study design

We used a two-gate case-control design (Holtman et al., 2019), in which confirmed ALS patients were recruited alongside healthy controls as an early stage trial to study the potential of MUMRI as a

diagnostic test. Ten ALS patients were recruited from a specialist ALS clinic, with ten age-comparable healthy controls recruited via advertisement within the university and local newsletters between March 2021 to October 2021. Inclusion criteria for ALS patients were diagnosis with definite or probable motor neuron disease based on the Awaji-Shima criteria (de Carvalho et al., 2008). Exclusion criteria were contra-indications for MRI, inability to lie flat, and advanced disease (ALS Functional Rating Scale [ALSF-RS] < 25, forced vital capacity [FVC] < 60%, non-invasive ventilation or receiving percutaneous gastrostomy feeding). For healthy controls, participants had to be older than 45 years of age to ensure a similar age range to the ALS patients. Exclusion criteria were history of neuromuscular disease, contra-indications to MRI and inability to lie flat. The study was approved by the Medical Ethics Committee Wales REC 5 (ref 19/WA/0279) and Newcastle University Ethics Committee (ref 1808/14610/2019). All participants underwent an MRI examination and SEMG examination at baseline and the ALS patients underwent the same examinations again 6 months later. Participant characteristics were collected at baseline, including ALS-FRS and FVC for the ALS patients.

2.2. Data acquisition

2.2.1. MRI examination

Each participant underwent an MRI examination of the lower leg muscles, paraspinal muscles, biceps brachii and tongue using a 3 T Achieva X MR Scanner (Philips Medical Systems, Best, The Netherlands). First, the tongue, paraspinal muscles and lower leg muscles were examined. The participant lay supine and was positioned head first in the scanner, with padding under the knees and ankles to ensure the calves were suspended with a relaxed muscle position to minimize volitional motor unit activity. A combination of a 15-channel head coil, 16-channel posterior spine coil and 16-channel torso coil were used. Thereafter, the participant was repositioned towards the side of the scanner bore with the right upper arm relaxed and as close to centre of the bore as possible. A pair of 10 cm elliptical receive coils were then positioned around the upper arm. The image slices were positioned at mid-line tongue, midline of biceps brachii for the arm, the thickest part of the calf for the lower leg muscles and the intervertebral disc in between L3-L4 for the paraspinal muscles.

For each body region, fasciculation was imaged with a PGSE sequence. We acquired 180 repetitions of four slices per body region with the diffusion encoding direction alternating between right-left, anterior-posterior and feet-head. For the tongue, the 180 repetitions were split into two sets of 90 repetitions to minimise the time that the participant needed to keep the tongue relaxed. In between the two acquisition sets, the subject was allowed to swallow. This resulted in 720 images per body region, subdivided into 60 images per slice and diffusion encoding direction. For the lower leg muscles, biceps brachii and paraspinal muscles, the PGSE setting for motion sensitivity (*b*-value) was set at $b = 200 \text{ s/mm}^2$, while for the tongue $b = 20 \text{ s/mm}^2$ was chosen to reduce sensitivity and minimise detection of volitional tongue muscle activation. Table 1 provides details on sequence parameters. Per body region, two repetitions with $b = 0 \text{ s/mm}^2$ (insensitive for fasciculation) were also acquired to allow image registration. The lower leg muscles, tongue and paraspinal muscles were imaged bilaterally and the biceps brachii unilaterally (right-side). The duration of MUMRI sequences was 12 minutes in total; 3 minutes per body region.

2.2.2. SEMG examination

Fasciculation rates were also examined with conventional single-channel SEMG for the right biceps brachii and right soleus. The active and inactive electrodes (Ambu, Copenhagen, Denmark)

were positioned according to the SENIAM guidelines (The SENIAM project). For the biceps brachii, the recording electrodes were placed 20 mm apart on the line between the medial acromion and the cubital fossa at 1/3 from the cubital fossa, and the reference electrode was placed at the lateral side of the humerus. For the soleus, the recording electrodes were placed 20 mm apart at 2/3 of the line between the medial condyle of the femur to the medial malleolus, and the reference electrode was placed on the medial malleolus. The soleus was chosen in accordance with the SENIAM guidelines recommending to record from this muscle in supine position, equivalent to the data collection scanning position used for the MUMRI acquisition in the lower legs.

Recordings were made in a room adjacent to the scanner and were performed within 60 minutes of the MRI scans. SEMG recording were performed with a Biopac MP150 acquisition system (BIO-PAC System Inc., Goleta, United States) and AcqKnowledge software (version 4.4). Gain was set to 5000 and high pass and low pass filter set at 1 Hz and 5 kHz, respectively.

To reproduce the position during the MRI examination, the participant lay supine with both arms positioned relaxed next to the body. If needed, a pillow was placed under the knees to minimize volitional motor unit activity. Once volitional motor unit activity was minimized in both the biceps brachii and the soleus according to the SEMG trace, up to 10 minutes of resting SEMG data was acquired.

2.3. Data-processing and analysis

2.3.1. MRI data

All images were analysed using custom-written scripts in Matlab (version R2019a, MathWorks Natick, MA, USA). For fasciculation detection, all PGSE images were registered to their corresponding $b = 0$ s/mm² image using rigid registration. The muscle tissue was manually delineated (Fig. 1A). The lower leg muscles included the tibialis anterior and extensor digitorum (TA), peroneus longus (PER), tibialis posterior (TP), gastrocnemius medialis (GM), gastrocnemius lateralis (GL) and the soleus (SOL). The paraspinal muscles were segmented in the lower back images and the biceps brachii in the upper arm images. The triceps was not examined because it was often located at the edge of the scanner bore resulting in a failed main magnetic field shim and consequently highly distorted muscle with poor fat suppression. The tongue tissue was segmented from the tip of the tongue towards the base of the tongue, using sagittal T1-weighted images as reference.

Within the segmented muscle tissue, transient signal voids were detected with a custom-written algorithm (Fig. 1B/C). The time-series of each voxel was first normalized to its baseline signal, with baseline defined as the 75th percentile over the whole time-series in that voxel. A signal void was then defined as a group of connected voxels where the signal intensity dropped to a value smaller than 0.6. The minimum signal void size was set at 10 mm², because this was the minimum motor unit size found in previous work (Birkbeck et al., 2020; Heskamp et al., 2022). Each diffusion encoding direction and the two acquisitions of the tongue were analysed separately, because the baseline signal differed between the three directions and the tongue position varied between the two subsequent blocks.

We counted the number of detected signal voids per body region and defined this as the number of fasciculations. The MUMRI fasciculation rate, measured in cm⁻³min⁻¹, was calculated as the number of fasciculations normalised to the sampled muscle volume and acquisition time. The change over 6 months' time was calculated as the difference between the follow-up MUMRI fasciculation rate minus the baseline MUMRI fasciculation rate.

2.3.2. SEMG data

The SEMG data was also analysed with Matlab. The bipolar SEMG traces were filtered with a 50 Hz notch filter, including harmonics at 100, 150, and 200 Hz. Thereafter, a 3-minute window with minimum voluntary activity and artefacts was selected. The number of fasciculations was counted using the Surface Potential Quantification Engine (SPiQE) algorithm (Bashford et al., 2019). This identifies spikes based on a probabilistic analysis of spikes relative to the baseline noise. The probability threshold was set at 98% and the spike amplitude detection threshold was set at 6 times the spike specific noise level around a potential spike. Spikes were excluded as volitional activity if at least 4 consecutive spikes appeared within 250 ms of each other. SEMG fasciculation rate was defined as the number of detected spikes divided by the acquisition time. The change over 6 months' time was again defined as the follow-up SEMG fasciculation rate minus the baseline SEMG fasciculation rate.

2.4. Statistical analysis

Statistical analysis was performed using IBM SPSS Statistics for Windows (version 28, Armonk, NY, USA). For group-comparisons, parametric tests were applied for normally distributed data and non-parametric tests for non-normally distributed data.

The baseline MUMRI and SEMG fasciculation rates were compared between ALS patients and healthy controls for each body region using a Mann-Whitney U test. Longitudinal changes in MUMRI and SEMG fasciculation rates were examined with a one-sample t-test. All tests were Bonferroni corrected for the number of examined body regions.

To propose the use of MUMRI as a putative diagnostic tool for ALS, it is important to assess if the detected fasciculation rate in a muscle of an individual ALS patient deviates from the rate observed in a healthy control population. To test this in our study population, the fasciculation rate of each muscle or body region of ALS patients was expressed as a z-score, using the healthy control values as reference:

$$z - score = \frac{\text{Fasciculation rate participant} - \text{mean}(\text{fasciculation rate healthy controls})}{\text{standard deviation}(\text{fasciculation rate healthy controls})}$$

We defined a fasciculation rate as abnormally increased when the z-score was greater than 3 (equals $p = 0.040$ after Bonferroni correction for 15 different muscles). This analysis was performed for both MUMRI and SEMG fasciculation rates.

The relation between MUMRI fasciculation rates and SEMG fasciculation rates were examined with a Spearman correlation.

Statistical significance was set at $p < 0.05$. Data are presented as mean \pm standard deviation (SD), unless stated otherwise.

2.5. Data availability statement

The data that support the findings of this study are available from the corresponding author, upon reasonable request.

3. Results

3.1. Participants

We included ten patients (64 ± 7 years, 3 female) and ten healthy controls (58 ± 10 years, 3 female). In order to reflect an unscreened clinical population we included any ALS sub-type. Nine patients were diagnosed with typical ALS phenotype (both upper and lower motor neuron signs; $n = 9$), of whom two had bulbar onset and seven had limb onset. One patient (P10) was diagnosed with primary lateral sclerosis (PLS; only upper motor neuron signs) (Table 2).

Table 1
Sequence settings of the motor unit MRI (MUMRI) pulsed gradient spin-echo (PGSE) sequence for each body region.

| Body region | Tongue | Biceps brachii | Paraspinals | Lower legs |
|------------------------------|--|---|---|---|
| Participant position | Head first supine | Head first supine | Head first supine | Head first supine |
| Coil | 15-channel head coil (Philips) | Pair of 10 cm elliptical surface coil (Philips) | 16-channel posterior spine coil (Philips) | 16-channel Torso coil (Philips) + 16-channel posterior spine coil (Philips) |
| Orientation | sagittal | transversal | transversal | transversal |
| Field of view (mm) | 192 × 128 | 144 × 144 | 256 × 120 | 384 × 168 |
| In-plane resolution (mm) | 2 × 2 | 1.5 × 1.5 | 2 × 2 | 2 × 2 |
| Slice thickness/gap (mm) | 8/0 | 10/0 | 10/5 | 10/5 |
| b-value (s/mm ²) | 20 | 200 | 200 | 200 |
| Δ/δ (ms) | 15.6/6.5 | 22.6/6.5 | 23.9/6.5 | 19.4/6.5 |
| Diffusion direction* | FH, AP, RL | RL, AP, FH | RL, AP, FH | RL, AP, FH |
| TR/TE (ms) | 1050/33 | 1100/47 | 1125/49 | 1050/38 |
| Number of dynamics | 180 | 180 | 180 | 180 |
| Fat suppression technique | SPAIR + SSGR | SPAIR + SSGR + OFS | SPAIR + SSGR + OFS | SPAIR + SSGR + OFS |
| Total acquisition time | 3:15 min [#] | 3:21 min | 3:25 min | 3:12 min |
| Other settings | 80 mm saturation slab positioned posterior | | Phase Oversampling of 168 mm Anterior | |

* Diffusion sensitization direction was alternated (i.e. RL, AP, FH, RL, AP, FH etc).

[#] The tongue images were acquired in two separate blocks to allow the participants to swallow in between the two blocks. RL: Right-Left, AP: Anterior-Posterior, FH; Feet-Head, TR: Repetition time, TE = echo time, SPAIR = Spectral Attenuated Inversion Recovery, SSGR = Slice Selective Gradient Reversal, OFS = Olefinic Fat Suppression

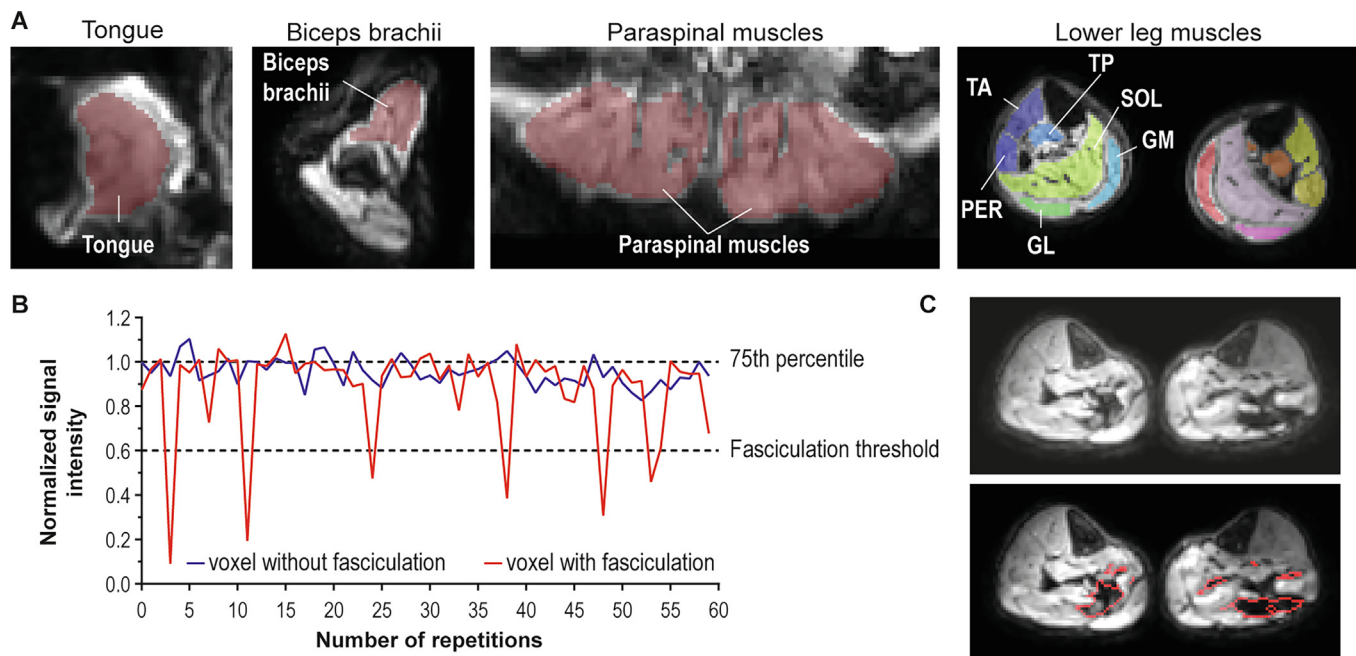


Fig. 1. Data-processing pipeline. A) Examples of diffusion weighted images with their manual muscle segmentation overlaid in colour for the tongue, biceps brachii, paraspinal muscles, and lower leg muscles. B) Fasciculation detection algorithm showing the time-series of a voxel normalized to the 75% percentile of the whole time-series in an area demonstrating fasciculation (red) and an area demonstrating no fasciculation (blue). The voxel in the fasciculating area shows 6 fasciculations (signal intensity < 0.6). C) Example of the detected signal voids at a single time-point delineated in red. GL = Gastrocnemius lateralis, GM = gastrocnemius medialis, PER = peroneus longus, SOL = Soleus, TA = tibialis anterior + extensor digitorum, TP = tibialis posterior.

The ALS patients did not differ from the healthy controls in age ($p = 0.123$), sex ($p = 0.876$) or BMI ($p = 0.786$) (Table 2). Median time from diagnosis of the ALS patients was 26 months (range: 1 to 65 months), and their mean ALS-FRS and FVC were 42 ± 4 and $96 \pm 20\%$, respectively.

One ALS patient (P9) did not attend the follow-up visit due to loss of ambulation. Furthermore, 5 out of 80 MUMRI datasets were excluded at baseline, i.e. two upper arm datasets (1 ALS and 1 healthy, because of an inhomogeneous magnetic field at the edge of the bore), one paraspinal dataset (healthy, because of image artefact from breathing) and two tongue datasets (1 ALS and 1 healthy, due to excess volitional activity). We excluded one base-

line SEMG biceps brachii dataset (PLS) because of excess volitional activity.

3.2. Baseline – ALS patients vs. healthy controls

3.2.1. MUMRI fasciculation rates

Healthy controls showed no or minimal fasciculation in each body region (Fig. 2A). The patient with PLS also showed no increased fasciculation (Fig. 2B; P10). Therefore, we performed subsequent group analysis on the ten healthy controls vs. the nine typical ALS patients and present the PLS patient as a separate case.

All nine patients with the typical ALS phenotype presented with a high number of fasciculations in at least one body region (Fig. 2A/B). The regions with increased fasciculation were not always adjacent; for example in patient P2, increased fasciculation was detected in the tongue and lower legs but not in the arms or paraspinal muscles. Videos of the DW images corresponding to the displayed motor unit activity maps can be found in supplemental video 1.

The MUMRI fasciculation rate did not differ between the three diffusion encoding directions, therefore we combined the data into one MUMRI fasciculation rate over all three diffusion directions. At group-level, the MUMRI fasciculation rate in ALS patients was higher compared to healthy controls for the biceps brachii ($2.40 \pm 1.90 \text{ cm}^{-3}\text{min}^{-1}$ vs. $0.04 \pm 0.10 \text{ cm}^{-3}\text{min}^{-1}$, $p = 0.004$), paraspinal muscles ($1.14 \pm 1.61 \text{ cm}^{-3}\text{min}^{-1}$ vs. $0.02 \pm 0.02 \text{ cm}^{-3}\text{min}^{-1}$, $p = 0.016$) and lower leg muscles ($1.42 \pm 1.27 \text{ cm}^{-3}\text{min}^{-1}$ vs. $0.13 \pm 0.10 \text{ cm}^{-3}\text{min}^{-1}$, $p = 0.004$), but not in the tongue ($1.41 \pm 1.94 \text{ cm}^{-3}\text{min}^{-1}$ vs. $0.18 \pm 0.18 \text{ cm}^{-3}\text{min}^{-1}$, $p = 0.556$) (Fig. 3A and Table 3). The fasciculation rate observed in an individual muscle of a healthy control ranged from no observed fasciculation to a maximum of $0.86 \text{ cm}^{-3}\text{min}^{-1}$ with on average the soleus and gastrocnemius having the highest mean fasciculation rates and the tibialis anterior the lowest fasciculation rates (Fig. 3B, Supplemental Table 1). In ALS, this range was much larger, from no observed fasciculations up to $11.59 \text{ cm}^{-3}\text{min}^{-1}$ (tibialis posterior).

To assess the potential diagnostic value of MUMRI at the individual patient level, we displayed the MUMRI fasciculation rate in each ALS patient relative to the distribution of MUMRI fasciculation rates in healthy controls (z-score) for each individual muscle and body region (Fig. 2B/3C). We used a stringent threshold of $z = 3$ that minimizes the chance of classifying a body region with elevated fasciculation rates in healthy controls. With this threshold, for MUMRI, 9/9 of the ALS patients had an increased fasciculation rate (z-score > 3) in at least 1 body region and 6/9 ALS patients in at least two body regions. Three ALS patient showed increased fasciculation in only one muscle at baseline (P4: biceps brachii; P6 and P7: lower legs). Of the two patients with bulbar onset disease, one (P5) showed an increased fasciculation rate in the tongue whereas the other did not (P7).

3.2.2. SEMG fasciculation rates and its relation with MUMRI

At group-level, SEMG fasciculation rate in the biceps brachii differed between ALS patients and healthy controls ($13.15 \pm 11.08 \text{ min}^{-1}$ vs. $3.24 \pm 4.00 \text{ min}^{-1}$, $p = 0.034$). The soleus demonstrated fasciculation in both ALS patients and healthy controls, with no difference between the two groups ($34.78 \pm 37.61 \text{ min}^{-1}$ vs. 22.79 ± 20.56 , $p > 0.999$) (Fig. 4A and Table 3). At group level, the MUMRI fasciculation rate correlated with SEMG fasciculation rate ($\tau = 0.475$, $p = 0.006$) (Fig. 4B). This correlation was mainly driven by the biceps brachii.

Individual patient analysis by expressing the fasciculation rate as a z-score showed that 4/9 typical ALS patients had an increased SEMG fasciculation rate in the right soleus or biceps brachii (Fig. 4C). By contrast, 9/9 ALS patients showed an increased fasciculation rate in these muscles detected by MUMRI. The patient diagnosed with PLS had normal fasciculation rates on both SEMG and MUMRI. In one patient (P2), SEMG showed an increased fasciculation rate in the biceps brachii, while MUMRI did not.

3.3. Change in fasciculation rate over 6 months in ALS patients

3.3.1. MUMRI fasciculation rates

In total 8 typical ALS patients and the PLS patient were examined at both visit 1 and visit 2. The average follow-up time was 6.0 ± 0.3 months. In 7 of those patients all 4 body regions were examined and in 2 patients 3 body regions were examined, i.e. a

total of 34 body regions were studied. In typical ALS patients, all 18 body regions with increased MUMRI fasciculation rates at baseline still had elevated MUMRI fasciculation rates after 6 months (Fig. 2B/5A). In 5 typical ALS patients, a body region with a normal MUMRI fasciculation rate at baseline converted into an increased MUMRI fasciculation rate (z-score > 3) at 6 months follow-up (1 biceps brachii, 1 lower legs, 3 paraspinals, all encircled in green in Fig. 5A). This included the three patients (P4, P6 and P7) who had a single body region with increased fasciculation at baseline. Hence at follow-up, 8/8 typical ALS patients had an increased fasciculation rate in two body regions. Interestingly, in P6, the region that developed fasciculation at follow-up (right arm) was not contiguous with the region present at baseline (leg) since the paraspinal region remained unaffected. The time of diagnosis was 4 months for P4, 55 months for P6 and 65 months for P7. As expected, the PLS patient (P10) continued to show normal fasciculation rates. At group level, the MUMRI fasciculation rate did not change over 6 months' time in any of the body regions of the ALS patients (all muscle groups $p > 0.999$; Table 3).

3.3.2. SEMG fasciculation rates and its relation with MUMRI

The biceps brachii of two ALS patients changed from a normal appearing SEMG fasciculation rate at baseline to a significantly increased SEMG fasciculation rate at 6-month follow-up (green circles; Fig. 5B). One biceps brachii and two soleus muscles showed a change in the opposite direction, from an elevated SEMG fasciculation rate at baseline to a normal appearing SEMG fasciculation rate at follow-up (red squares). In line with MUMRI, ALS patients showed no significant change in group-level SEMG fasciculation rate over 6 months' time (both muscles $p > 0.999$) (Table 3). The longitudinal change in fasciculation rate did not correlate between MUMRI and SEMG ($\tau = 0.230$, $p = 0.234$) (Fig. 5C).

4. Discussion

MUMRI detected a more than 10-fold elevation in fasciculation rate in the biceps brachii, lumbar paraspinal muscles and lower leg muscles of typical ALS patients compared to healthy controls. Fasciculation in the biceps brachii or paraspinal muscles was most specific for ALS, as those muscles showed hardly any fasciculation in healthy controls (mean rate $< 0.05 \text{ min}^{-1}\text{cm}^{-2}$). This is in line with recent ultrasound studies that assessed up to ~ 20 muscles and showed that the presence of fasciculation in thoracic and proximal limb muscles was most specific for ALS diagnosis (Fukushima et al., 2022; Johansson et al., 2017; Liu et al., 2021; Tsuji et al., 2017).

In our study, the fasciculation rate in the tongue could not discriminate ALS patient from healthy controls. This was also the case in the two patients who presented with bulbar symptoms, one of whom showed significantly raised fasciculation in the tongue with the other patient showing no increase. The lack of discrimination was largely due to the high variation in fasciculation rates in healthy controls. This high variability is likely caused by the high sensitivity of MUMRI to muscle contraction in combination with the difficulty of relaxing the tongue. As a consequence MUMRI detects even minor volitional tongue motion. Despite this limitation, both patients with bulbar onset ALS showed increased fasciculation in at least 1 body regions at baseline.

We wanted to reflect the population being seen in a specialist ALS clinic and to that end included patients with any variety of ALS including predominantly upper-motor neuron forms. Unsurprisingly, the one patient with primary lateral sclerosis did not show increased fasciculation rates at either baseline or follow-up.

In our study, 6/9 of the typical ALS patients fulfilled the Gold Coast criteria for denervation based on MUMRI at baseline and

Table 2
Baseline demographics.

| | Healthy controls (n = 10) | Typical ALS patients (n = 9) | p-value | PLS patient (n = 1) |
|-----------------------------------|------------------------------|---------------------------------|---------|------------------------|
| Age (years) | 58 ± 10 | 64 ± 7 | 0.123 | 66 |
| Sex | | | 0.876 | |
| Female, n (%) | 3 (33%) | 3 (30%) | | - |
| Male, n (%) | 6 (67%) | 7 (70%) | | 1 (100%) |
| BMI (kg/m ²) | 25.2 ± 4.2 | 24.6 ± 4.4 | 0.786 | 22.5 |
| Phenotype | | | | |
| Spinal onset, n (%) | | 7 (78%) | | |
| Bulbar onset, n (%) | | 2 (22%) | | |
| Time since diagnosis (months) | | 20 ± 23 | | 33 |
| Time since symptom onset (months) | | 43 ± 48 | | 111 |
| ALS FRS | | 42 ± 4 | | 42 |
| FVC (%) | | 96 ± 20 | | 69 |

All data are presented as mean ± SD. ALS = Amyotrophic lateral sclerosis. PLS = Primary lateral sclerosis. BMI = body mass index. ALS FRS = ALS Functional rating scale. FVC = forced vital capacity.

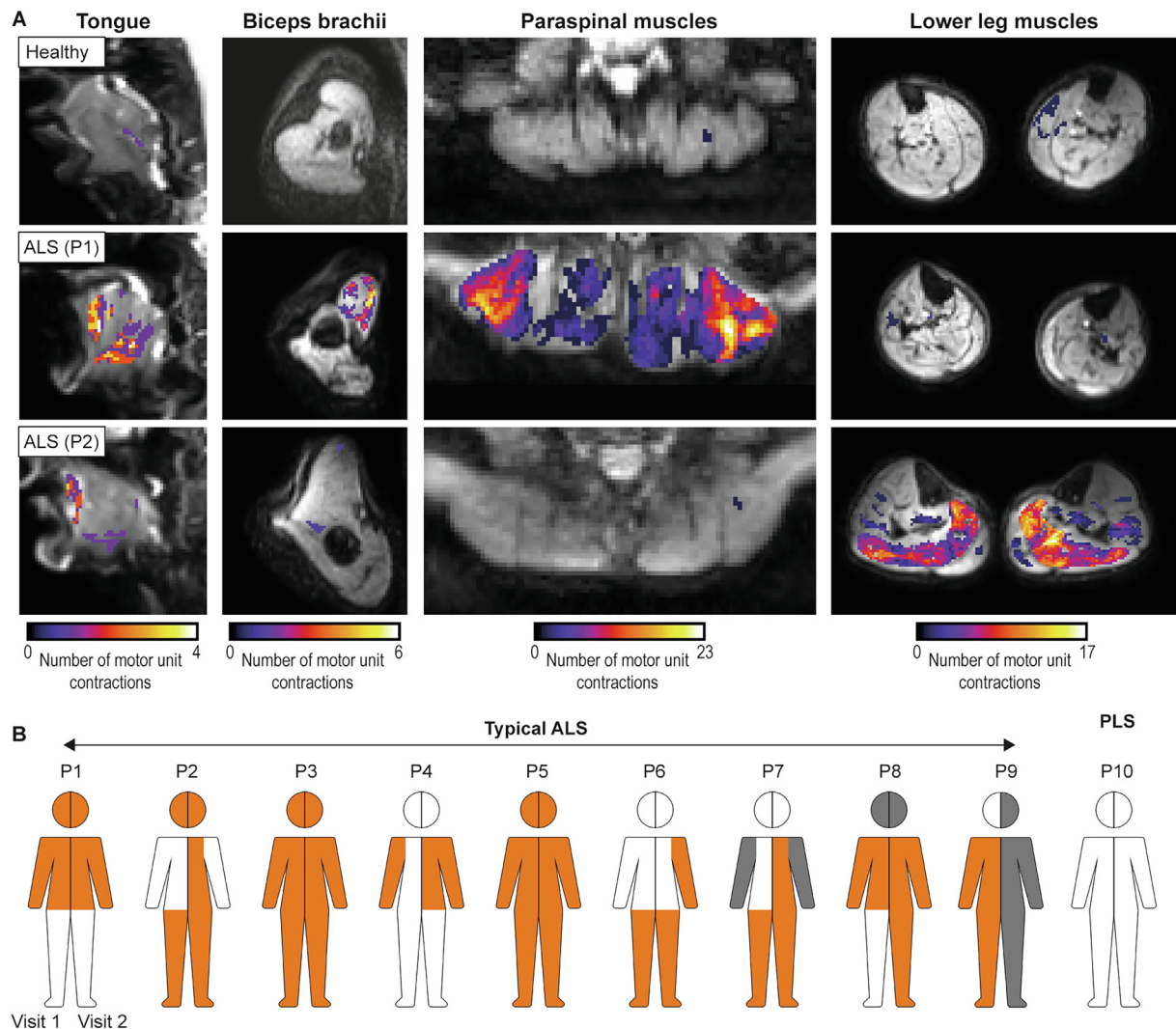


Fig. 2. Typical examples motor unit activity maps and schematic overview of the results. A) Motor unit activity maps are created for feet-head diffusion encoding direction by summing the number of fasciculations detected per voxel. This included 60 repetitions for the biceps brachii, paraspinal muscles and lower legs muscles and 30 repetitions (1 block) for the tongue. Top: The healthy control shows almost no fasciculation on the motor unit MRI (MUMRI) images in any body region. Middle: Amyotrophic lateral sclerosis (ALS) patient (P1) shows fasciculation on the MUMRI images of the tongue, biceps brachii and paraspinal muscles, while almost no fasciculation is seen in the lower leg muscles. Bottom: ALS patient (P2) with severe fasciculation on the MUMRI images of the lower leg muscles and some fasciculation in the tongue, and little or no fasciculation being detected on the images of the other body regions. See supplemental video for the diffusion weighted images corresponding to these motor unit activity maps. B) Schematic representation of the study results with the left and the right side of the body representing visit 1 and visit 2 respectively. P10 is diagnosed with primary lateral sclerosis (PLS) and all other patients are diagnosed with typical ALS phenotype. Body regions with a fasciculation rate in the range of healthy controls (z -score < 3) are displayed in white and body region with an increased fasciculation rate (z -score > 3) in orange. Missing data is displayed in grey.

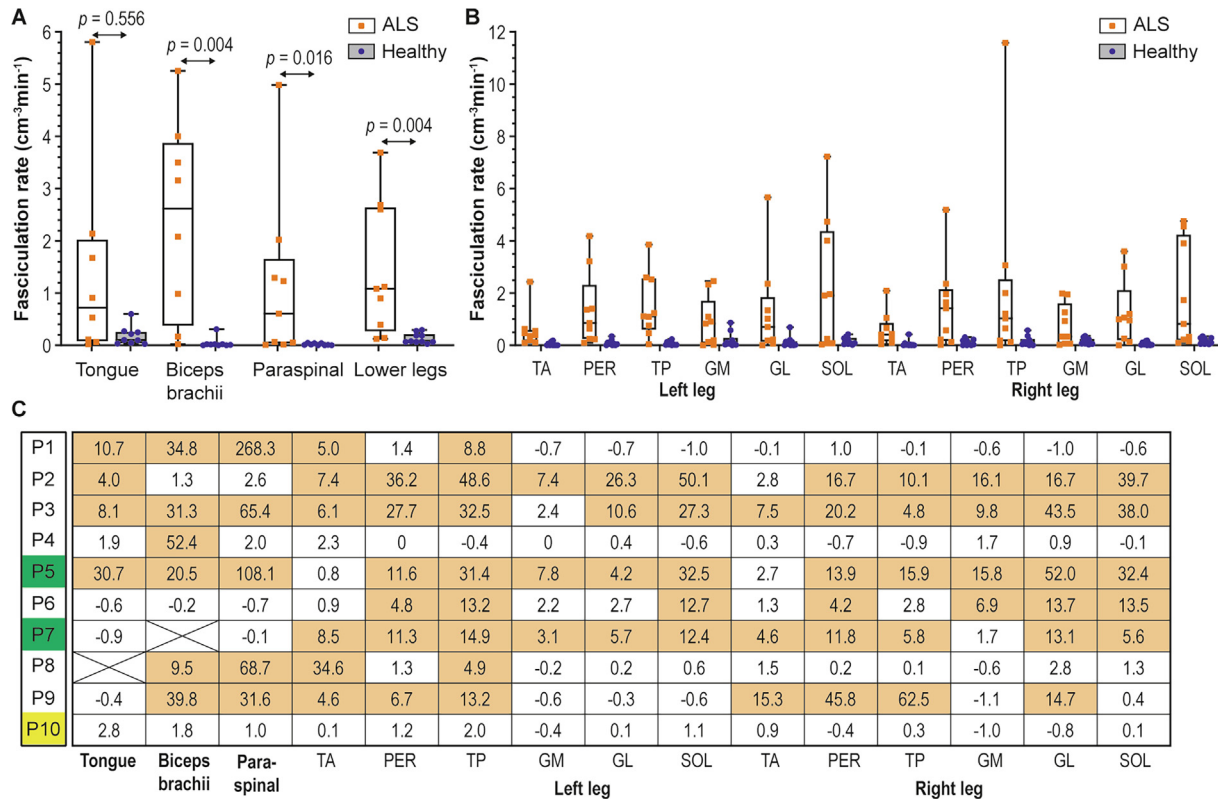


Fig. 3. Motor unit MRI (MUMRI) baseline fasciculation rates in amyotrophic lateral sclerosis (ALS) patients compared to healthy controls. A) MUMRI fasciculation rate in typical ALS patients vs. healthy controls for the tongue, biceps brachii, paraspinal muscles, and lower leg muscles. B) MUMRI fasciculation rate in typical ALS patients vs. healthy controls for individual lower leg muscles. C) MUMRI fasciculation rate in the 9 typical ALS patients (P1-P9) and the primary lateral sclerosis (PLS) patient (P10) per muscle relative to the healthy controls expressed in the z-score. Muscles with a fasciculation rate in the range of healthy controls (z -score < 3) are displayed in white cells and muscles with an increased fasciculation rate (z -score > 3) are displayed in orange cells. The number within the cell is the z-score. Crossed regions reflect missing data. The two ALS patients who presented with bulbar onset are highlighted in green, and the PLS patient is highlighted in yellow.

Table 3

Motor unit MRI (MUMRI) and surface EMG (SEMG) fasciculation rates in ten healthy controls vs. nine typical amyotrophic lateral sclerosis (ALS) patients and one primary lateral sclerosis (PLS) patient at baseline and their change over six months' time.

| | Healthy controls | | Typical ALS patients | | p-value | PLS patient | |
|---|------------------|------------------------------|----------------------|------------------------------|------------------|-------------|-------|
| | n | Value | n | Value | | n | Value |
| Baseline | | | | | | | |
| MUMRI number of fasciculations | | | | | | | |
| Tongue | 9 | 32 ± 34; 17 [38] | 8 | 181 ± 231; 120 [240] | 0.800 | 1 | 58 |
| Biceps brachii | 9 | 8 ± 19; 3 [5] | 8 | 220 ± 177; 194 [293] | <0.001 | 1 | 35 |
| Paraspinal muscles | 9 | 9 ± 9; 4 [14] | 9 | 431 ± 713; 187 [530] | 0.044 | 1 | 11 |
| Lower leg muscles | 10 | 172 ± 119; 111 [202] | 9 | 1568 ± 1411; 1417 [2289] | 0.012 | 1 | 185 |
| MUMRI Fasciculation rate (cm³·min⁻¹) | | | | | | | |
| Tongue | 9 | 0.18 ± 0.18; 0.10 [0.22] | 8 | 1.41 ± 1.94; 0.72 [1.95] | 0.556 | 1 | 0.70 |
| Biceps brachii | 9 | 0.04 ± 0.10; 0.02 [0.03] | 8 | 2.40 ± 1.90; 2.62 [3.50] | 0.004 | 1 | 0.23 |
| Paraspinal muscles | 9 | 0.02 ± 0.02; 0.01 [0.04] | 9 | 1.14 ± 1.61; 0.60 [1.62] | 0.016 | 1 | 0.04 |
| Lower leg muscles | 10 | 0.13 ± 0.10; 0.08 [0.15] | 9 | 1.42 ± 1.27; 1.08 [2.38] | 0.004 | 1 | 0.16 |
| SEMG Fasciculation rate (min⁻¹) | | | | | | | |
| Biceps brachii | 10 | 3.24 ± 4.00; 2.00 [2.33] | 9 | 13.15 ± 11.08; 10.67 [18.83] | 0.034 | 1 | NA |
| Soleus | 10 | 22.79 ± 20.56; 18.00 [19.68] | 9 | 34.78 ± 37.61; 20.33 [70.17] | >0.999 | 1 | 3.67 |
| Change over 6 month's time | | | | | | | |
| MUMRI Fasciculation rate (cm³·min⁻¹) | | | | | | | |
| Tongue | | | 7 | 0.13 ± 1.16; -0.02 [1.15] | >0.999 | 1 | -0.22 |
| Biceps brachii | | | 7 | 0.69 ± 1.95; 0.45 [4.54] | >0.999 | 1 | -0.15 |
| Paraspinal muscles | | | 8 | -0.28 ± 1.36; 0.07 [0.84] | >0.999 | 1 | 0.01 |
| Lower leg muscles | | | 8 | 0.24 ± 2.27; 0.03 [0.99] | >0.999 | 1 | 0.02 |
| SEMG Fasciculation rate (min⁻¹) | | | | | | | |
| Biceps brachii | | | 8 | 5.46 ± 20.26; -0.84 [34.09] | >0.999 | 1 | NA |
| Soleus | | | 8 | -0.54 ± 32.66; -1.84 [12.75] | >0.999 | 1 | NA |

All data is presented as mean ± SD; median [interquartile range]. Outcome measures were compared with a Mann-Whitney U test for ALS vs. healthy and one-sample t-test for longitudinal changes in ALS patients. All reported p-values are Bonferroni corrected to the number of body regions examined (n = 4 for MUMRI and n = 2 for SEMG). NA equals missing data in the PLS patient.

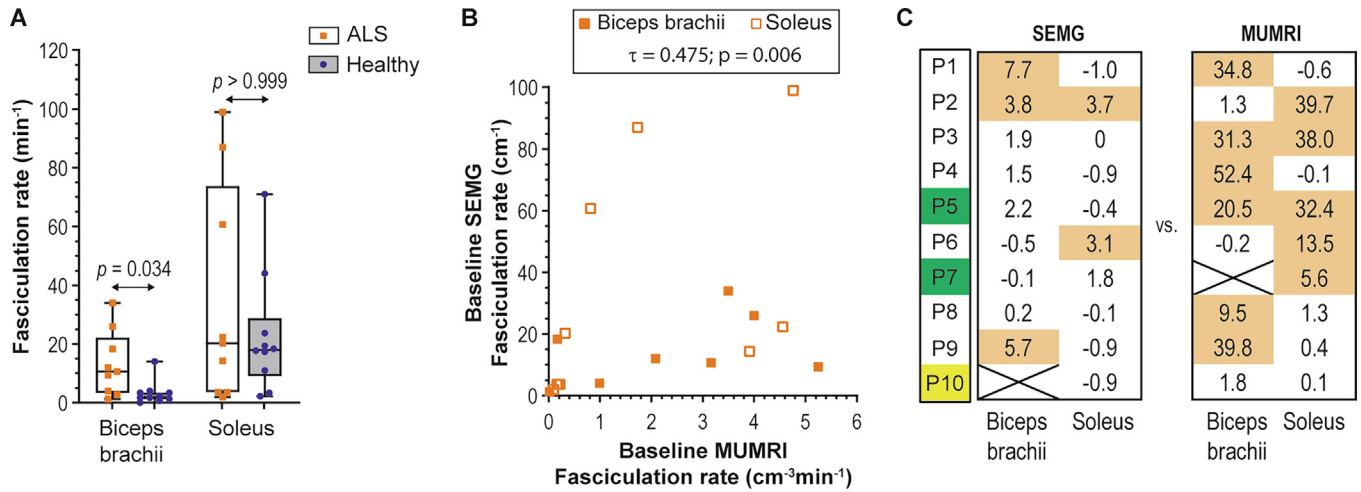


Fig. 4. Surface EMG (SEMG) baseline fasciculation rates in amyotrophic lateral sclerosis (ALS) patients compared to healthy controls. A) SEMG fasciculation rate in typical ALS patients vs. healthy controls in the biceps brachii and soleus. B) Correlation between MUMRI fasciculation rate and SEMG fasciculation rate. C) SEMG fasciculation rate in the 9 typical ALS patients (P1-P9) and the primary lateral sclerosis (PLS) patient (P10) for the biceps and soleus relative to the healthy controls expressed in the z-score, displayed against the z-score of these muscles for MUMRI. Muscles with a fasciculation rate in the range of healthy controls (z-score < 3) are displayed in white cells and muscles with an increased fasciculation rate (z-score > 3) are displayed in orange cells. The number within the cell is the z-score. Crossed regions reflect missing data. The two ALS patients who presented with bulbar onset are highlighted in green, and the PLS patient is highlighted in yellow.

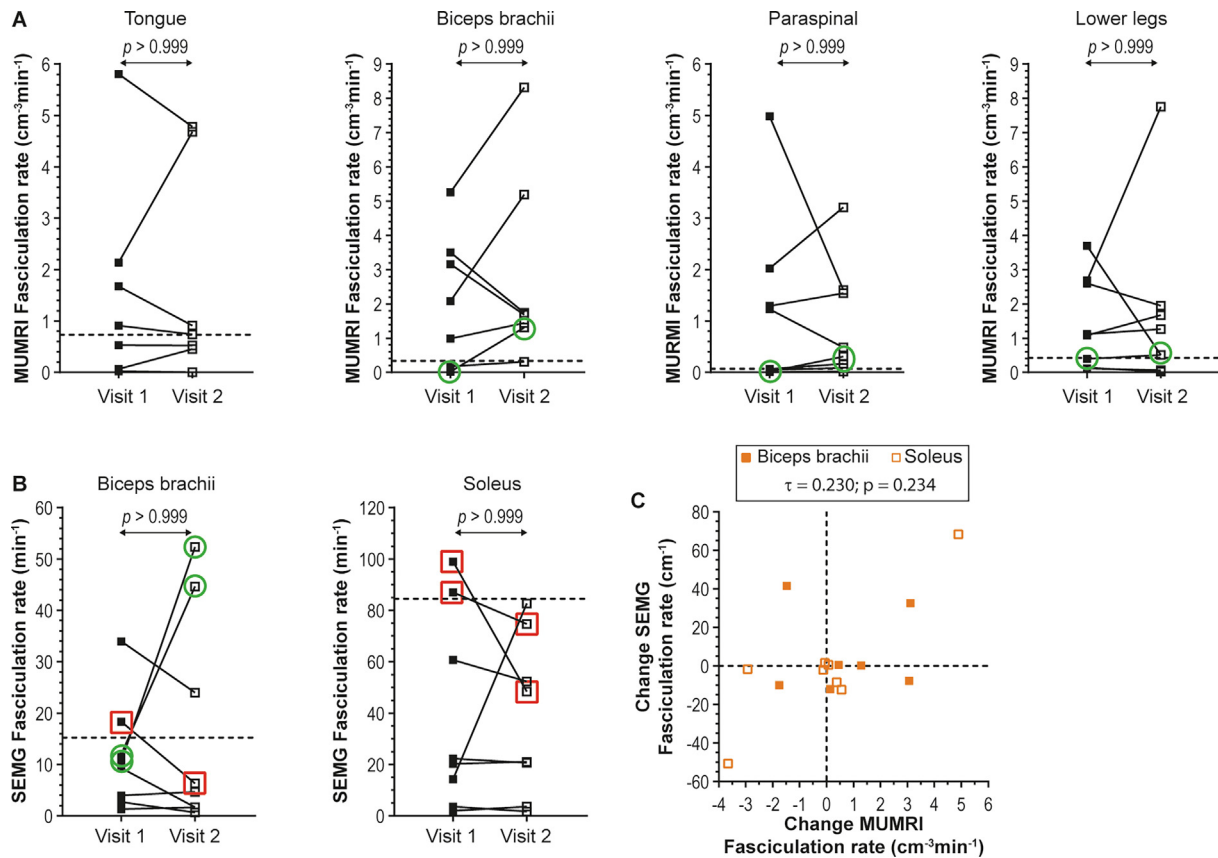


Fig. 5. Six-month change in fasciculation rates in amyotrophic lateral sclerosis (ALS) patients for motor unit MRI (MUMRI) and surface EMG (SEMG). A) Change in MUMRI fasciculation rate for the tongue, biceps brachii, paraspinal muscles, and lower legs of the typical ALS patients. The dotted line equals the $z = 3$ of the healthy control distribution of MUMRI fasciculation rates. Patients in which a muscle or muscle group had a normal appearing MUMRI fasciculation rate at baseline (z-score < 3) and an elevated MUMRI fasciculation rate at follow-up (z-score > 3) are depicted with green circles. B) Change in SEMG fasciculation rate for the biceps brachii and soleus of the typical ALS patients. Patients in which a muscle changed from normal appearing SEMG fasciculation rate to an elevated SEMG fasciculation rate, or in opposite direction are depicted in green circles or red squares, respectively. C) Correlation between change in MUMRI fasciculation rate and change in SEMG fasciculation rate.

8/8 of the typical ALS patients supported those criteria at follow-up, *i.e.* they showed fasciculation in at least 2 body regions. The three patients that only met the Gold Coast criteria at follow-up were relatively early in the disease process (4 months post diagnosis at baseline visit) or very late after diagnosis (55 and 65 months post diagnosis at baseline visit), compared to the average time from diagnosis of 20 months in the 9 typical-ALS patients (ranging from 1 to 65 months).

Overall, the sensitivity to detect fasciculation was higher with MUMRI compared to single channel SEMG applied in our study, probably due to much larger coverage with MUMRI. Furthermore, whereas fasciculation rates fell back to normal in some muscles on SEMG, MUMRI fasciculation rates appeared to increase steadily with disease progression. It should be noted that the MUMRI and SEMG were not performed simultaneously (although they were within 60 minutes of each other) and the fasciculation rate is known to be variable over time. However, high density SEMG measurements performed at 3 time point in a single day (9 am, 12 noon and 3 pm) showed a consistent fasciculation rate during the day for the biceps with an intraclass correlation coefficient of 95% (confidence interval: 85% to 99%) (Bashford et al., 2020). Furthermore, it is worth mentioning that a single channel EMG method was used as this is currently the most commonly available technique for clinical neurophysiologists. This technique has been shown to outperform clinical observation when it comes to fasciculation detection (Hjorth et al., 1973; Howard and Murray, 1992; Mateen et al., 2008), but is also known to be less sensitive than multi-channel SEMG (Tamborska et al., 2020). For example, fasciculation rates in biceps brachii assessed with a 64-channel SEMG grid could discriminate ALS patients from patients with alternative possible diagnosis and healthy controls with 80% sensitivity and 96% specificity (Tamborska et al., 2020).

As with other diagnostic algorithms for ALS, the Gold Coast criteria divide the body into four regions. Diagnosis requires the combination of an appropriate clinical history (progressive muscle weakness), evidence of upper- and lower-motor neuron involvement in one body region, or lower-motor neuron involvement in two. It also requires the exclusion of alternative diagnoses, which typically includes some form of imaging. Hence, the diagnosis rests on multiple convergent pieces of evidence, which no single test can provide. Perhaps needle EMG comes closest, in that it can provide evidence of both denervation and re-innervation in the same muscle, albeit in an invasive and relatively time-consuming procedure.

Ultrasound is readily available and is increasingly used in routine clinical care for fasciculation detection. It has a sensitivity of 86% and specificity of 96% when fasciculation is detected in 3 or more of the following 8 muscles: trapezius, tongue, biceps brachii, flexor digitorum, rectus abdominis, vastus medialis and soleus (Fukushima et al., 2022). It remains to be seen how MUMRI compares in terms of diagnostic sensitivity and specificity, as well as user acceptability. Similarly to the earliest ultrasound studies on fasciculation detection (Grimm et al., 2015), our study has now shown that MUMRI can discriminate diagnosed ALS patients from healthy controls. Our MUMRI data therefore support the need to conduct a larger study that should include people with alternative possible diagnoses to ALS and ultrasound as an additional measure to fully understand the potential role of MUMRI.

MUMRI has some potential advantages. Firstly, MUMRI fasciculation scanning can be combined with complimentary assessments of motor unit loss, such as fat infiltration, atrophy and acute denervation (STIR +) not readily detectable by ultrasound. Second, it has a large coverage area and can assess superficial and deep muscles with equal sensitivity, *e.g.* 14 lower leg muscles can be examined in a single 3 minute scan (Kriss and Jenkins, 2022). It is also worth noting that the MUMRI sequence (PGSE) is commonly available on any clinical MRI scanners and that 8 out of the 10 included

patients had already undergone MRI imaging as part of their diagnostic work-up. Some Centres perform MRI in all suspected ALS patients (Galvin et al., 2017; Turner et al., 2010). This suggests that MUMRI could provide sensitive whole-body fasciculation counting with relatively minor impact on the routine clinical imaging already being performed in these patients, providing complimentary information to needle EMG or potentially as a means of better targeting this to affected muscles.

For future work, the MUMRI protocol can be further optimized. Currently, we imaged four body regions with a 3-minute acquisition time per region. This allowed us to examine 15 individual muscles with 12 minutes of imaging time. The imaging time per body region could be shortened because the analysis of a single diffusion direction (1-minute) was equally sensitive to detect fasciculation and discriminate ALS patients from healthy controls when compared to full 3-minute acquisition including all three diffusion encoding directions. However, this needs to be examined systemically in a larger study cohort including, as shorter examination times may reduce diagnostic sensitivity.

The main limitations of the present study are the sample size and the inclusion criteria of patients with an already established ALS diagnosis. Furthermore, the patients in our study had a relatively long time since diagnosis (average 20 months), suggesting our patients were mainly slow progressors. The obvious next step is to apply MUMRI in a larger prospective study in people who are suspected of ALS in order to determine its sensitivity and specificity in this clinical setting.

In conclusion, motor unit MRI offers a novel non-invasive technique to image fasciculation in several muscle groups simultaneously. In this study, MUMRI detected an increased fasciculation rate in at least 2 body regions for 6/9 patients at baseline and 8/8 patients at follow-up. The MUMRI fasciculation rate correlated well with the single-channel SEMG fasciculation rate. Discrimination by MUMRI between ALS patients and healthy controls was best demonstrated in the proximal limb muscles (biceps brachii) and thoracic region (paraspinal muscles), whereas the tongue could not discriminate the two groups. Future studies should therefore include imaging of other bulbar muscles and upper leg muscles. We see MUMRI as a potentially useful adjunct to current diagnostic tests, which can be easily combined with the structural imaging that the vast majority of suspected ALS patients already undergo.

CRediT authorship contribution statement

Linda Heskamp: Conceptualization, Resources, Software, Data Curation, Formal Analysis, Investigation, Writing – original draft, Writing – review & editing, Visualization, Project Administration, Funding acquisition. **Matthew G. Birkbeck:** Conceptualization, Software, Writing – review & editing. **Julie Hall:** Conceptualization, Writing – review & editing. **Ian.S. Schofield:** Software. **James Bashford:** Conceptualization, Writing – review & editing. **Timothy L. Williams:** Conceptualization, Resources, Writing – review & editing. **Hugo M. De Oliveira:** Conceptualization, Resources, Writing – review & editing. **Roger G. Whittaker:** Conceptualization, Writing – review & editing, Supervision, Funding acquisition. **Andrew M. Blamire:** Conceptualization, Software, Writing – review & editing, Supervision, Funding acquisition.

Funding

This work was supported by the Rubicon research programme (project number: 452183002) of the Dutch Research Council (Nederlandse Organisatie voor Wetenschappelijk Onderzoek (NWO)).

Acknowledgements

We would like to thank all participants for their participation and the radiographers for their help with the data-acquisition. Furthermore, we acknowledge the use of the Fat-Water Toolbox (<http://isrmr.org/workshops/FatWater12/data.htm>) for some of the results shown in this article. The SPiQE analytical toolkit for SEMG was developed through funding support from the Medical Research Council, Motor Neuron Disease Association and National Institute for Health and Care Research (<https://www.kcl.ac.uk/spiqe>).

Conflict of interest

The authors report no conflict of interests.

Author contributions

The experiments were performed by L.H. All authors were involved in the conception and design of the work. L.H., T.L.W. and H.M.O. recruited the participants. L.H., M.G.B., I.S.S., and A.M. B. developed the MUMRI data-analysis pipeline and J.B. developed the SEMG data-analysis pipeline. L.H. processed all the data. All authors were involved in interpretation of the data. L.H. wrote the first draft. All authors were involved in revising the manuscript.

Appendix A. Supplementary data

Supplementary data to this article can be found online at <https://doi.org/10.1016/j.clinph.2024.02.016>.

References

- Bashford J, Masood U, Wickham A, Iniesta R, Drakakis E, Boutelle M, et al. Fasciculations demonstrate daytime consistency in amyotrophic lateral sclerosis. *Muscle Nerve* 2020;61:745–50. <https://doi.org/10.1002/mus.26864>.
- Bashford J, Wickham A, Iniesta R, Drakakis E, Boutelle M, Mills K, et al. SPiQE: An automated analytical tool for detecting and characterising fasciculations in amyotrophic lateral sclerosis. *Clin Neurophysiol* 2019;130:1083–90. <https://doi.org/10.1016/j.clinph.2019.03.032>.
- Birkbeck MG, Heskamp L, Schofield IS, Blamire AM, Whittaker RG. Non-invasive imaging of single human motor units. *Clin Neurophysiol* 2020;131:1399–406. <https://doi.org/10.1016/j.clinph.2020.02.004>.
- de Carvalho M, Dengler R, Eisen A, England JD, Kaji R, Kimura J, et al. Electrodiagnostic criteria for diagnosis of ALS. *Clin Neurophysiol* 2008;119:497–503. <https://doi.org/10.1016/j.clinph.2007.09.143>.
- de Carvalho M, Kiernan MC, Swash M. Fasciculation in amyotrophic lateral sclerosis: origin and pathophysiological relevance. *J Neurol Neurosurg Psychiatry* 2017;88:773–9. <https://doi.org/10.1136/jnnp-2017-315574>.
- de Carvalho M, Swash M. Fasciculation discharge frequency in amyotrophic lateral sclerosis and related disorders. *Clin Neurophysiol* 2016;127:2257–62. <https://doi.org/10.1016/j.clinph.2016.02.011>.
- de Carvalho M, Swash M. Fasciculation potentials and earliest changes in motor unit physiology in ALS. *J Neurol Neurosurg Psychiatry* 2013;84:963–8. <https://doi.org/10.1136/jnnp-2012-304545>.
- de Carvalho M, Turkman A, Pinto S, Swash M. Modulation of fasciculation frequency in amyotrophic lateral sclerosis: Table 1. *J Neurol Neurosurg Psychiatry* 2015; jnnp-2014-309686. <https://doi.org/10.1136/jnnp-2014-309686>.
- Feldman EL, Goutman SA, Petri S, Mazzini L, Savelieff MG, Shaw PJ, et al. Amyotrophic lateral sclerosis. *Lancet* 2022;400:1363–80. [https://doi.org/10.1016/S0140-6736\(22\)01272-7](https://doi.org/10.1016/S0140-6736(22)01272-7).
- Fukushima K, Takamatsu N, Yamamoto Y, Yamazaki H, Yoshida T, Osaki Y, et al. Early diagnosis of amyotrophic lateral sclerosis based on fasciculations in muscle ultrasonography: A machine learning approach. *Clin Neurophysiol* 2022;140:136–44. <https://doi.org/10.1016/j.clinph.2022.06.005>.
- Galvin M, Ryan P, Maguire S, Heverin M, Madden C, Vajda A, et al. The path to specialist multidisciplinary care in amyotrophic lateral sclerosis: A population-based study of consultations, interventions and costs. *PLoS One* 2017;12:e0179796.
- Grimm A, Prell T, Décard BF, Schumacher U, Witte OW, Axer H, et al. Muscle ultrasonography as an additional diagnostic tool for the diagnosis of amyotrophic lateral sclerosis. *Clin Neurophysiol* 2015;126:820–7. <https://doi.org/10.1016/j.clinph.2014.06.052>.
- Hardiman O, van den Berg LH, Kiernan MC. Clinical diagnosis and management of amyotrophic lateral sclerosis. *Nat Rev Neurol* 2011;7:639–49. <https://doi.org/10.1038/nrneurol.2011.153>.
- Heskamp L, Miller AR, Birkbeck MG, Hall J, Schofield IS, Blamire AM, et al. In vivo 3D imaging of human motor units in upper and lower limb muscles. *Clin Neurophysiol* 2022. <https://doi.org/10.1016/j.clinph.2022.05.018>.
- Hjorth RJ, Walsh JC, Willison RG. The distribution and frequency of spontaneous fasciculations in motor neurone disease. *J Neurol Sci* 1973;18:469–74. [https://doi.org/10.1016/0022-510X\(73\)90140-8](https://doi.org/10.1016/0022-510X(73)90140-8).
- Hobson-Webb LD, Simmons Z. Ultrasound in the diagnosis and monitoring of amyotrophic lateral sclerosis: a review. *Muscle Nerve* 2019;60:114–23. <https://doi.org/10.1002/mus.26487>.
- Holtman GA, Berger MY, Burger H, Deeks JJ, Donner-Banzhoff N, Fanshawe TR, et al. Development of practical recommendations for diagnostic accuracy studies in low-prevalence situations. *J Clin Epidemiol* 2019;114:38–48. <https://doi.org/10.1016/j.jclinepi.2019.05.018>.
- Househam E, Swash M. Diagnostic delay in amyotrophic lateral sclerosis: what scope for improvement? *J Neurol Sci* 2000;180:76–81. [https://doi.org/10.1016/S0022-510X\(00\)00418-4](https://doi.org/10.1016/S0022-510X(00)00418-4).
- Howard RS, Murray NMF. Surface EMG in the recording of fasciculations. *Muscle Nerve* 1992;15:1240–5. <https://doi.org/10.1002/mus.880151104>.
- Johansson MT, Ellegaard HR, Tankisi H, Fuglsang-Frederiksen A, Qerama E. Fasciculations in nerve and muscle disorders – A prospective study of muscle ultrasound compared to electromyography. *Clin Neurophysiol* 2017;128:2250–7. <https://doi.org/10.1016/j.clinph.2017.08.031>.
- Kiernan MC, Vucic S, Cheah BC, Turner MR, Eisen A, Hardiman O, et al. Amyotrophic lateral sclerosis. *Lancet* 2011;377:942–55. [https://doi.org/10.1016/S0140-6736\(10\)61156-7](https://doi.org/10.1016/S0140-6736(10)61156-7).
- Kriss A, Jenkins T. Muscle MRI in motor neuron diseases: a systematic review. *Amyotroph Lateral Scler Frontotemporal Degener* 2022;23:161–75. <https://doi.org/10.1080/21678421.2021.1936062>.
- Liu J, Li Y, Niu J, Zhang L, Fan J, Guan Y, et al. Fasciculation differences between ALS and non-ALS patients: an ultrasound study. *BMC Neurol* 2021;21:441. <https://doi.org/10.1186/s12883-021-02473-5>.
- Mateen FJ, Sorenson EJ, Daube JR. Strength, physical activity, and fasciculations in patients with ALS. *Amyotroph Lateral Scler* 2008;9:120–1. <https://doi.org/10.1080/17482960701855864>.
- Misawa S, Noto Y, Shibuya K, Iose S, Sekiguchi Y, Nasu S, et al. Ultrasonographic detection of fasciculations markedly increases diagnostic sensitivity of ALS. *Neurology* 2011;77:1532–7. <https://doi.org/10.1212/WNL.0b013e318233b36a>.
- Paganoni S, Macklin EA, Lee A, Murphy A, Chang J, Zipf A, et al. Diagnostic timelines and delays in diagnosing amyotrophic lateral sclerosis (ALS). *Amyotroph Lateral Scler Frontotemporal Degener* 2014;15:453–6. <https://doi.org/10.3109/21678421.2014.903974>.
- Palese F, Sartori A, Logroscino G, Pisa FE. Predictors of diagnostic delay in amyotrophic lateral sclerosis: a cohort study based on administrative and electronic medical records data. *Amyotroph Lateral Scler Frontotemporal Degener* 2019;20:176–85. <https://doi.org/10.1080/21678421.2018.1550517>.
- Sennfält S, Kläppe U, Thams S, Samuelsson K, Press R, Fang F, et al. The path to diagnosis in ALS: delay, referrals, alternate diagnoses, and clinical progression. *Amyotroph Lateral Scler Frontotemporal Degener* 2022;1–9. <https://doi.org/10.1080/21678421.2022.2053722>.
- Shefner JM, Al-Chalabi A, Baker MR, Cui LY, de Carvalho M, Eisen A, et al. A proposal for new diagnostic criteria for ALS. *Clin Neurophysiol* 2020;131:1975–8. <https://doi.org/10.1016/j.clinph.2020.04.005>.
- Steidle G, Schick F. Addressing spontaneous signal voids in repetitive single-shot DWI of musculature: Spatial and temporal patterns in the calves of healthy volunteers and consideration of unintended muscle activities as underlying mechanism. *NMR Biomed* 2015;28:801–10. <https://doi.org/10.1002/nbm.3311>.
- Tamborska A, Bashford J, Wickham A, Iniesta R, Masood U, Cabassi C, et al. Non-invasive measurement of fasciculation frequency demonstrates diagnostic accuracy in amyotrophic lateral sclerosis. *Brain Commun* 2020;2:1–9. <https://doi.org/10.1093/braincomms/fcaa141>.
- Tsuji Y, Noto Y, Shiga K, Teramukai S, Nakagawa M, Mizuno T. A muscle ultrasound score in the diagnosis of amyotrophic lateral sclerosis. *Clin Neurophysiol* 2017;128:1069–74. <https://doi.org/10.1016/j.clinph.2017.02.015>.
- Turner MR, Scaber J, Goodfellow JA, Lord ME, Marsden R, Talbot K. The diagnostic pathway and prognosis in bulbar-onset amyotrophic lateral sclerosis. *J Neurol Sci* 2010;294:81–5. <https://doi.org/10.1016/j.jns.2010.03.028>.
- Westeneng H-J, Debray TPA, Visser AE, van Eijk RPA, Rooney JPK, Calvo A, et al. Prognosis for patients with amyotrophic lateral sclerosis: development and validation of a personalised prediction model. *Lancet Neurol* 2018;17:423–33. [https://doi.org/10.1016/S1474-4422\(18\)30089-9](https://doi.org/10.1016/S1474-4422(18)30089-9).
- Whittaker RG, Porcari P, Braz L, Williams TL, Schofield IS, Blamire AM. Functional magnetic resonance imaging of human motor unit fasciculation in amyotrophic lateral sclerosis. *Ann Neurol* 2019;85:455–9. <https://doi.org/10.1002/ana.25422>.